Surface modification of Co3O4 nanostructures using wide range of natural compounds from rotten apple juice for the efficient oxygen evolution reaction

Abdul Jaleel Laghari, Umair Aftab, Aqeel Ahmed Shah, Muhammad Yameen Solangi, Muhammad Ishaque Abro, Sameerah Al-Saeedi, Noha Naeim, Ayman Nafady, Brigitte Vigolo, Melanie Emo, et al.

Surface modification of Co_3O_4 nanostructures using wide range of natural compounds from rotten apple juice for the efficient oxygen evolution reaction

Abdul Jaleel Laghari[a], Umair Aftab[a], Aqeel Ahmed Shah[c], Muhammad Yameen Solangi[a], Muhammad Ishaque Abro[a], Sameerah I. Al-Saeedi[h], Noha Naeim[f], Ayman Nafady[g], Brigitte Vigolo[d], Melanie Emo[d], Antonia Infantes Molina[e], Aneela Tahira[b], Zafar Hussain Ibhupoto[b]*

[a]Department of Metallurgy and Materials Engineering, Mehran University of Engineering and Technology, 76080 Jamshoro, Sindh Pakistan

[b]Dr. M.A Kazi Institute of Chemistry University of Sindh Jamshoro, 76080, Sindh Pakistan

[c]Department of Metallurgy, NED university of Engineering and Technology, Karachi Pakistan

[d]Université de Lorraine, CNRS, IJL, F-54000 Nancy, France

[e]Department of Inorgnic Chemistry, Crystallography and Mineralogy. (Unidad Asociada al ICP-CSIC), Faculty of Sciences, University of Malaga, Campus de Teatinos, 29071 Malaga, Spain France

[f]Department of Production Engineering and Mechanical Design, Port Said University, Port Fua, 42526, Egypt

[g]Department of Chemistry, College of Science, King Saud University, Riyadh 11451, Saudi Arabia

[h]Department of Chemistry, College of Science, Princess Nourah bint Abdulrahman University, P.O.Box 84428, Riyadh 11671, Saudi Arabia

Corresponding authors: Zafar Hussian Ibupoto, PhD*, Email address: zaffar.ibhupoto@usindh.edu.pk

Abstract

In this study, a new strategy has been produced to use a rotten apple juice as a source for the surface modification of Co_3O_4 nanostructures, giving rise to efficient electro-catalysts for driving oxygen evolution reaction (OER) at relatively low over potential. We have studied the

morphology, chemical composition, and crystalline aspects of Co_3O_4 nanostructures using different analytical techniques. The Co_3O_4 nanostructures grown with rotten apple juice were observed with low impurity of Fe and P, surface modification, reduced particle size, high concentration of oxygen vacancies, defects and cubic phase of Co_3O_4. Furthermore, we have used the surface modified Co_3O_4 nanostructures for water electrolysis and noticed the significant performance towards OER in alkaline conditions. The electrochemical characterization revealed that the Co_3O_4 nanostructure prepared with 20 mL of rotten apple juice exhibits an overpotential value of 269 mV at 20 mA/cm^2 current density. The charge transport resistance (Rct) at the interface was estimated around 118.9 Ω, confirming an excellent reaction kinetics on the Co_3O_4 nanostructures and highly supported efficient performance towards OER. The Co_3O_4 nanostructures prepared with 20 mL of rotten apple juice has shown an acceptable durability for 40 h, verifying the long-term use. The performance of Co_3O_4 nanostructures with apple juice could be attributed to high oxygen vacancies due to high density of Co^{2+} ions on the surface, impurities of Fe and P, reduced nanoparticle size, defects in the structures, and favorable chemical composition. At the end, surface modified Co_3O_4 nanostructures was observed as an outperformed electrocatalyst when prepared with rotten apple juice. Therefore, this can be used in diverse purposes including energy conversion and storage applications.

Keywords: Rotten apple juice, Natural reducing agents, Co_3O_4 nanostructures, Oxygen evolution reaction

1. Introduction

In 2008, world energy consumption was approximately 11306.83 Mtoe and it has been increased about 13864.9 Mtoe in 2018 with a significant difference of 255.8 Mtoe/year [1]. For this reason, United Nations postulated the sustainable goals for renewable energy [2]. Therefore, the production of renewable energy resources has been grown successfully among various forms like solar [3], hydro [4], geothermal [5], bio waste [6], fuel cell [7-8] etc. Fuel cell development has gotten much attention because of higher efficiency, low capital cost, durable [9] and can be used directly for various purposes such as automotive [10-11] and electricity generation [12]. The development of efficient fuel cells, we need high amount of green fuels like hydrogen (H_2) and oxygen (O_2) [9-12]. The hydrogen gas is considered a high-density fuel compare to that of gasoline and methane [13], however there is no free avaiablity of hydrogen gas in nature. Hydrogen production from various chemical compounds has been carried out, however it

requires high energy demand and consequently the hydrogen production seems very costly [14]. Hence, researchers are focused on the hydrogen production from simple and toxic free environment, especially water splitting. Hydrogen generation from water dissociation is found to be the most efficient, environment friendly and renewable technology. Thermodynamically, 1.23 V energy is required to produce half mole of hydrogen gas from water molecule, this is an enormous amount of energy. Therefore, scientists are investigating large number of electrocatalysts to lower this energy barrier and bring it close to minimum potential value [15-19]. Currently, hydrogen production approximately 4% is obtained from water electrolysis [20], this low amount of hydrgen genration from water splititn is mainly associated to high energy demand and cost. Furthermore, water splitting involves two parallel processes: hydrogen evolution reaction (HER) at cathode and oxygen evolution reaction (OER) at anode. The HER is followed by two electron transfer and OER involves four electrons transfer process. Another challenging aspect for the efficient production of hydrogen gas from water splitting is due to difficulty of four electron transfer during OER process and it is known as a bottleneck barrier for the complete exploitation of hydrogen generation from water splitting to date. To overcome this barrier, an efficient OER electrocatalyst is need of immediate time for active and complete successful water catalysis process. At the moment, OER process is mainly characterized by the noble materials based electrocatalysts such as ruthenium oxide (RuO_2), palladium oxide (PdO) and Iridium oxide (IrO_2) [21,22,16], however their noble and scared nature is a big barrier to capitalize them for large scale water electrocatalysis. Thus, various nonprecious and earth abundant OER electrocatalysts have been developed including metal chalcogenide [23], metal hydroxide [24], metal phosphide [25], nano-carbons [26] and metal oxides [22] etc. The transition metal based electrocatalysts, particularly metal oxides of Sc, Ti, V, Cr, Mn, Fe, Co, Ni, Cu, and Zn [27-29] are found to be catalytically active due to partial electronic view of d-subshell [17].

Among them, cobalt oxide (Co_3O_4) is a low cost, earth abundant, environment friendly and exhibiting a spinel like crystal structure governed by mixed oxidation states of Co^{2+} and Co^{3+} enabling it as a strong candidate for the development of new generation of Co_3O_4 based OER electrocatalysts [30-32, 33-36]. After knowing the scientific uniqueness and attarctive aspects of d subshell electronic environment Co in Co_3O_4, and its prodctuon from earth abudnant materials, that makes the curisou researcherfs to investigate and enhance its perforamnec toarwds

electrochemcla reactions. Howeevr, its perfroamnce is limited by several factors such as poor chemisrption, durability issue, and low catalytic actvitiy. The extended research studies have been carried out to address the weak aspects of Co_3O_4, through improvement in crystal arrays, morphology and adapting specific synthetic strategies [22,37-39]. The reducing agents like glucose, sucrose, fructose, starch and ascorbic acids have been used previously during hydrothermal-combustion methods for tuning the physical and chemical properties of Co_3O_4 nanostructures [40-45]. Numerous methods have been used to prepare nanostructured materials like mechanical milling [46-48], co-precipitation [46-48], hydrothermal [47-52] and biological [48-53]. Among them, the biomass waste based synthetic approach is green, low cost and involve minimum toxic chemical compounds for tuning the functionality of nanostructured materials [48-52] . Different parts of plants have been studied like leaf, root, latex, seed, and stem during the synthesis of various nanostructured materials [50-52]. The =plant extracts offer the wide range of favorable chemical compounds like flavonoids, saponin and different phenolic with chelating/ reducing/ capping agent properties. They have been found highly useful to control on the size and dimension of different nanostructured materials [50-64]. Very surprisingly 1.3 million biomass waste of apple is being thrown away every year and the rotten apple his high source of rare iron and phosphorous dopant and containing the variety of naturally reducing agents. Hence, it has been wasted since long time irrespective of its favorable chemistry for tuning the functional properties of nanostructured materials. The rotten apple juice not only contains Fe/P but is rich with many of the reducing agents like glucose, sucrose, starch, polyphenols and ascorbic acid [65], and they can be considered as potential candidates for the surface modification of nanostructured electrocatalysts. The presented approach of using rotten apple juice is green and innovative, and it could be of great interest for enhancing the performance of a wide range of nanostructured materials.

It has been shown that the chemistry of fresh apple and rotten apple is almost same.

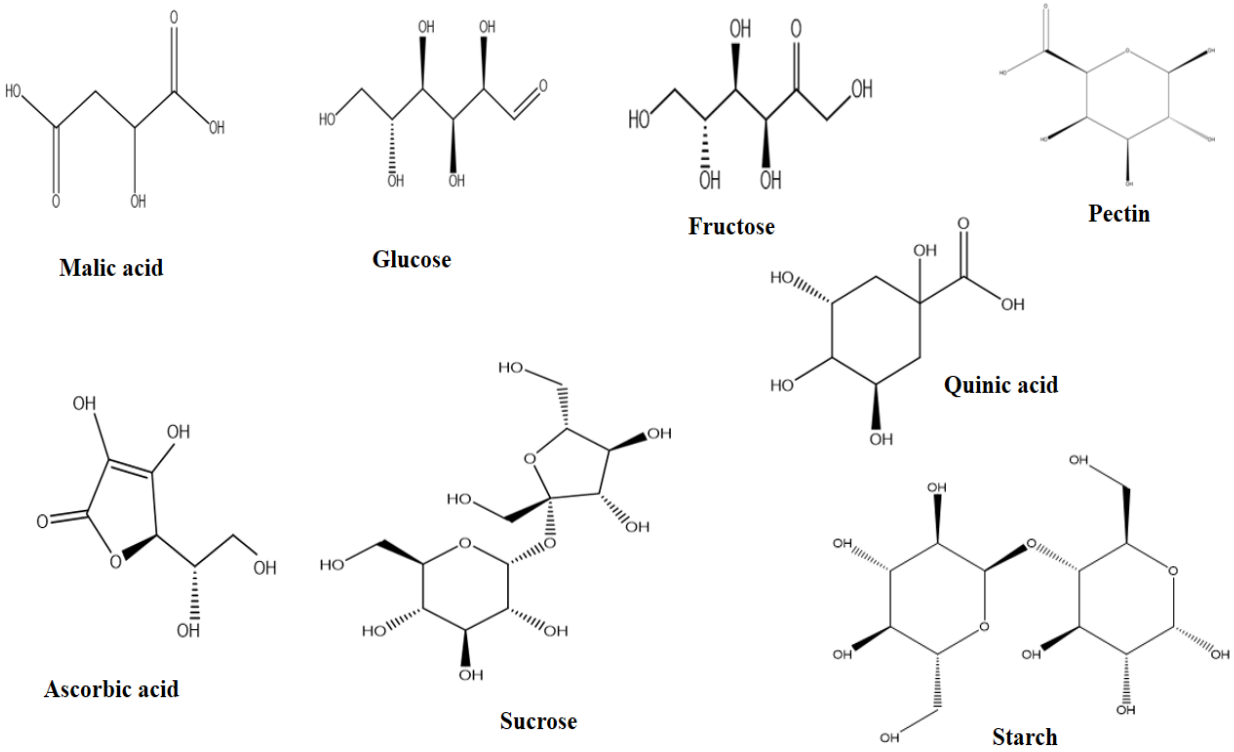

Figure 1: Main reducing constituents of rotten apple juice with their chemical structural view

Keeping the importance of green energy, unique features of Co_3O_4, and useful aspects of green synthesis, we have focused on the surface modification of Co_3O_4 nanostructures using rotten apple juice. There is no work done on the use of rotten apple juice for tailoring the surface based electrocatalytic properties of nanostructured Co_3O_4 material due to the presence of natural reducing agents such as glucose, sucrose, starch, polyphenols and ascorbic acid towards efficient OER reaction. Furthermore, the point of care in this study, we presented was the useful utilization of biomass waste of rotten apple juice. This is a natural raw material and it has potentially changed the catalytic properties of Co_3O_4 nanostructures and contributed its alternative role by lowering the cost of fabrication of material, limited the high use of toxic chemicals, involving the eco and environment friendly nature. The biomolecules carried by the rotten apple juice are associated with high density of oxygenated groups which could effectively modify the surface of Co_3O_4 nanostructures, consequently an enhanced OER activity is expected. Such aspects of rotten apple juice were not studied for the enhancement of catalytic properties of any nanostructured material and we for the first time realized and exploited theses beneficial

aspects of rotten apple juice for the development of improved Co_3O_4 based electrocatalyst for the OER half-cell reaction of water splitting.

In this study, we have used green approach of biomass waste of rotten apple juice for surface modification of Co_3O_4 nanostructures using hydrothermal method. We have studied the surface chemical composition, morphology, crystal arrays, and OER aspects of produced Co_3O_4 nanostructures. The doped Co_3O_4 nanostructures with iron and phosphorus with the volume of 20 mL of rotten apple juice has demonstrated an overpotential of 269 mV at 20 $mAcm^{-2}$ and it has been observed highly durable for 40 h.

2. Experimental Section

2.1 Materials

Cobalt chloride hexahydrate ($CoCl_2.6H_2O$), rotten apple juice, urea ($CH_4\ N_2\ O$), 85% potassium hydroxide (KOH), alumina 3µm (Al_2O_3) slurry, 20%ethanol (C_2H_5OH), and silicon paper, purchased from Sigma Aldrich Karachi, Sindh Pakistan. The desired solutions related to material synthesis and electrolyte were prepared in the deionized water.

2.2. Synthesis of surface modified Co_3O_4 nanostructures using rotten apple juice

The preparation of surface modified Co_3O_4 nanostructures was done with the use of various volumes of rotten apple juice by hydrothermal method. In a typical synthesis, 0.1M cobalt chloride hexahydrate and urea were mixed in 250 mL of deionized water. To optimize the effect of rotten apple juice, three separate beakers were taken and 0.1M cobalt and urea precursors were added in each beaker and different volumes of rotten apple juice (20, 20, and 30 mL) were added. They were labelled as cobalt apple (CA) with different volume of rotten apple juice (CA-10, CA-20 and CA-30) samples. Similarly, a beaker containing 0.1M cobalt and urea precursors was also used without rotten apple juice, and labeled as pristine Co_3O_4 nanostructures sample. The hydrothermal reaction was performed on these growth solutions covered with an aluminum sheet at 95 ^oC for 5h in an electric oven. Finally, the cobalt hydroxide product with pink color was collected on to an ordinary filter paper, washed several times with ethanol followed by deionized water and dried for overnight at 60 ^oC. For the collection of black color Co_3O_4 nanostructures, we performed the calcination at 500 ^oC for 3 h in air. Then, the pristine and

surface modified Co_3O_4 nanostructures with rotten apple juice were further used for different investigations like structural and electrochemical characterizations**.**

2.3.Structural and surface composition studies of surface modified Co_3O_4 nanostructures

The morphology of as ready nanomaterials was studied finished scanning electron microscopy (SEM) by JEOL JSM-6480A, operating voltage of 20kV, with (EDS) energy dispersive spectroscopy was functional to determine sample composition.

For finding the purity and crystalline phase of surface modified Co_3O_4 nanostructures, powder X-ray diffraction (XRD) was used (Philips PANanlytical) with CuKα radiation (λ = 1.5418 Å) was used as X-rays source, using 45 kV and current45 mA, and analysis was carried out with High score plus software [60,66]. **X-ray photoelectron spectroscopy (XPS)** was used for quantitative information about the chemical state and surface chemical composition of surface modified Co_3O_4 nanostructures using a model "the scienta ESCA 200" working through monochromatic x-ray source Al (k-alpha) of photons at 1486 eV under ultra-high vacuum using a pressure of 10^{-10} mbar. The obtained XPS experimental results were analyzed using 0.651 eV Auf 7/2 line of full width at half maximum. **Transmission electron microscopy** (TEM) was performed on a JEOL JEM ARM 200F-Cold FEG functional at 200 kV, equipped with spherical aberration (Cs).

2.4. Modification of glassy carbon electrode with surface modified Co_3O_4 nanostructures

All the electrochemical tests were done with VERSASTAT 4-500 analytical potentiostat using various electrochemical modes such as linear sweep voltammetry (LSV), cyclic voltammetry (CV), electrochemical impedance spectroscopy (EIS) and chronopotentiometry in 1.0 M KOH aqueous solution. Three electrode configurations were used for the electrochemical measurements. Glassy carbon electrode (GCE) as the working electrode, a silver-silver chloride (Ag/AgCl) filled with 3M potassium chloride solution (3MKCl) electrolyte as a reference electrode and a platinum wire as counter electrode. The Ag/AgCl was used in the glass rod and silver wire has no direct contact with alkaline electrolyte, hence the prevented by the effect of alkaline aqueous on the stability issue of reference electrode. We have applied large surface area of platinum wire of 0. 13cm^2. We have used low concentrated 1.0M KOH solution which has

less likely issues of instability for both the counter and reference electrodes. The catalyst dispersion of pristine and various surface modified Co_3O_4 nanostructures using rotten apple juice**,** and noble metal ruthenium oxide (RuO_2) for the modification of GCE was prepared by mixing 10 mg of each in 20 mL of deionized water with 0.3 mL of Nafion (5 %) and homogenous mixture was obtained in ultrasonic bath for stirring for 10-15 min. Alumina paste with silicon paper was used for the cleaning of GCE and GCE with a geometric area of 3 mm was used in the presented research work. The catalyst ink of 5 µL (0.02mg) was used to modify the surface of GCE and dried with the blow of air. The charge transfer resistance was measured by EIS with experimental conditions of 100 kHz to 0.1 Hz (as sweeping frequency range), sinusoidal potential of 5 mV and 1.4 V vs reversible hydrogen electrode (RHE) as a (OER Over-Potential). The raw EIS experimental data was further simulated by Z-view software in order to identify the right circuit to calculate accurate charge transfer resistance. The durability experiments very essential to confirm the performance evaluation of electrocatalyst for long term applications, therefore we did this measurement at conditions of current density of 20 mA/cm^{-2} for 40 h. The active surface area of electrocatalyst is very important for understanding the actual number of active sites involved in electrochemical reaction, hence cyclic voltammetry (CV) was adapted as method for this measurement at different scan rates. The electrochemical active surface area is represented by (ECSA) and the Nernst equation was used to transform experimental potential of reference (Ag/AgCl) electrode into reversible hydrogen electrode (RHE).

$$E_{RHE} = E_{Ag/AgCl} + 0.059pH + E^{o}_{Ag/AgCl} \quad (1)$$

Whereas $E^{o}_{Ag/Agcl}$ is 0.2412

$$Overpotential\ (\eta) = Onset\ potential\ (E_{RHE})_{(V)} - 1.23_{(V)} \quad (2)$$

Tafel equation was applied to LSV curves for the calculation of Tafel Slopes.

$$\eta = b \log j + a \quad (3)$$

Herein, b is Tafel slope, *ŋ overpotential* and *j is current density.*

3. Results and discussion

3.1. Structural and surface chemical composition analysis surface modified Co_3O_4 nanostructures using rotten apple juice

The phase purity of as synthesized Co_3O_4 nanostructures with different volumes of rotten apple juice were examined through powder XRD. Figure 2 shows the diffraction patterns of as synthesized Co_3O_4 nanostructures. The reflections of pristine Co_3O_4 nanostructures were well

matched with standard (JCPDS card no: 01-080-1534) and exhibiting cubic crystallography. The crystallographic planes of pristine Co_3O_4 were observed such as (220), (311), (222), (400), (511) and (440) at 2Ɵ angle of 31.139°, 36.556°, 38.384°, 44.612°, 59.082° and 64.929° respectively. The biomass waste assisted Co_3O_4 nanostructures including (samples CA-30, CA-20 and CA-10) have shown well defined diffraction patterns and they are in full agreement with the standard reference card (JCPDS card no: 01-080-1534). The measured diffraction patterns of rotten apple juice assisted Co3O4 nanostructures by XRD have shown slight two theta shift to right side due to induction of impurities of iron and P. Furthermore, the organic molecules present form the rotten apple juice during the crystal growth have created stressed which could be connected to the shift of two theta angle, consequently defects in the structure of Co_3O_4 were possibly found. The defects of crystal arrays changed the surface features of material, hence it could favor the reaction kinetics. The amount and nature of these defects within the Co_3O_4 nanostructures require additional studies in order to understand the role of them for lowering the overpotential during OER process. Moreover, after the calcination of prepared material at 500 ^oC for 5 hours, then all the organic stuff is removed from the surface of Co_3O_4. As it is already described that the organic molecules modified the surface of Co_3O_4 nanostructures during the growth process at certain limit due to their reducing nature, hence catalyst performance was also altered.

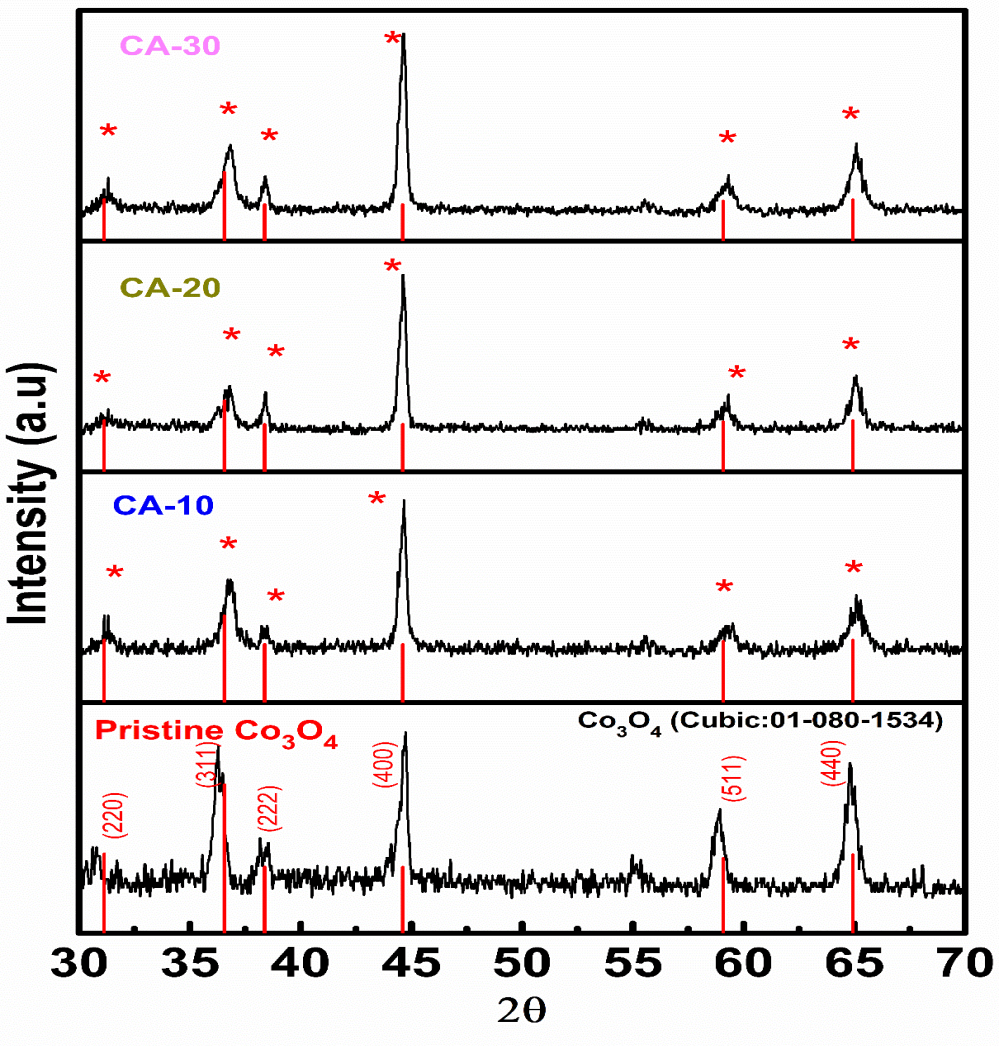

Figure 2: *XRD-pattern of pristine Co_3O_4, and rotten apple juice assisted Co_3O_4 nanostructures (CA-10, CA-20, and CA-30 samples).*

Figure 3 showing scanning electron microscopic (SEM) images analysis, was performed to explore the morphology of as grown Co_3O_4. Figure 3a shows pristine Co_3O_4 exhibits needle like shape with a porous structure. The use of 10 mL and 20 mL of rotten apple juice induces significant modification of Co_3O_4 nanostructures which appear as sea urchin-like structures (Figures 3 b to d). The presence of organic matter from rotten apple juice is revealed here to play a significant role in the Co_3O_4 growth mechanism and certainly acts as modifying surface agent

leading to strongly impact on the morphology of Co_3O_4 nanostructures. The reducing agents like glucose, sucrose, starch, polyphenols and ascorbic acid from rotten apple juice have dramatically transformed the morphology from needle like into aggregated and clusters of Co_3O_4 nanostructures. The presence of these types molecules during the growth process, suggesting that they have decreased the length of nanostructures and enabled the nucleation of to be grown particles and assembled them into aggregate and clustered morphology. Therefore, SEM study has revealed large impact of rotten apple juice on the morphology of Co_3O_4 from platelets to short range nanoparticles.

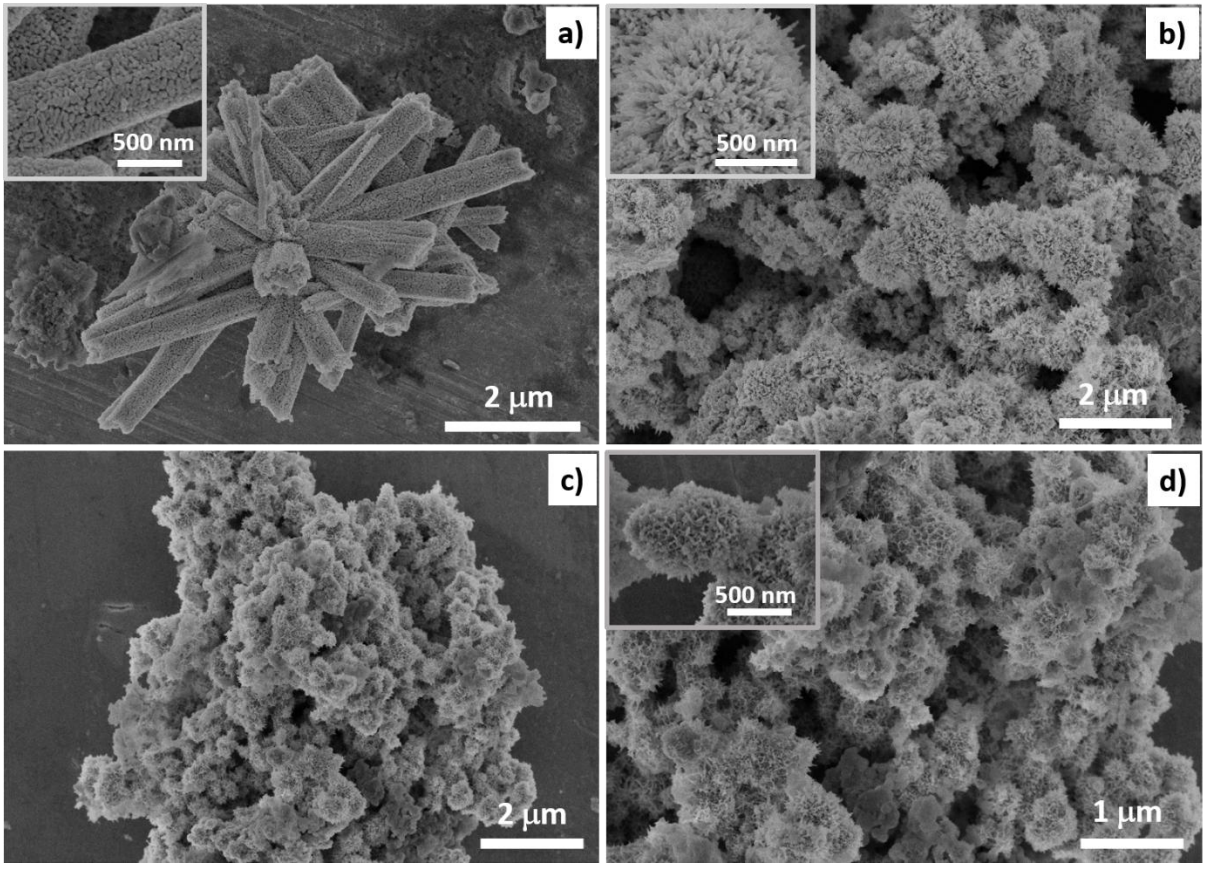

Figure 3: *Typical SEM images (a) pristine Co_3O_4 , (b) Co_3O_4 nanostructures with 10 mL (CA-10) of rotten apple juice, (c,d) Co_3O_4 nanostructures with 20 mL (CA-20) of rotten apple juice*

The complete structural, size and morphological properties of the samples were characterized by transmission electron microscopy (TEM). Figure 4 shows that pristine Co_3O_4 is composed of particles with diameter of 50-60 nm assembled in needle-like shape (Figures 4a-b) as already seen by SEM, while CA-20 is composed of aggregated particles with sizes between 6 and 20 nm (Figures 4e-g). Importantly, the particle size of Co_3O_4 is highly reduced with the use of rotten

apple juice, consequently swift OER kinetics is expected. Moreover, the EDX analyses indicating that the CA-20 sample contains also Fe and P as impurities in the sample (Figure 4h) compared to pure pristine Co_3O_4 (Figure 4d). Fast Fourier transforms (inserts of Figures 4c, f and g) present spots at 4.7, 2.8 and 2.4 Å, corresponding to (111), (220) and (311) planes of the cubic structure of Co_3O_4, as already shown by XRD experiments. Furthermore, the impurities of Fe was confirmed through EDX analysis, however additional presence of P was also observed. The presence of impurities of Fe and P in the chemical composition could have contribution towards the enhanced OER performance of as prepared Co_3O_4 nanostructures.

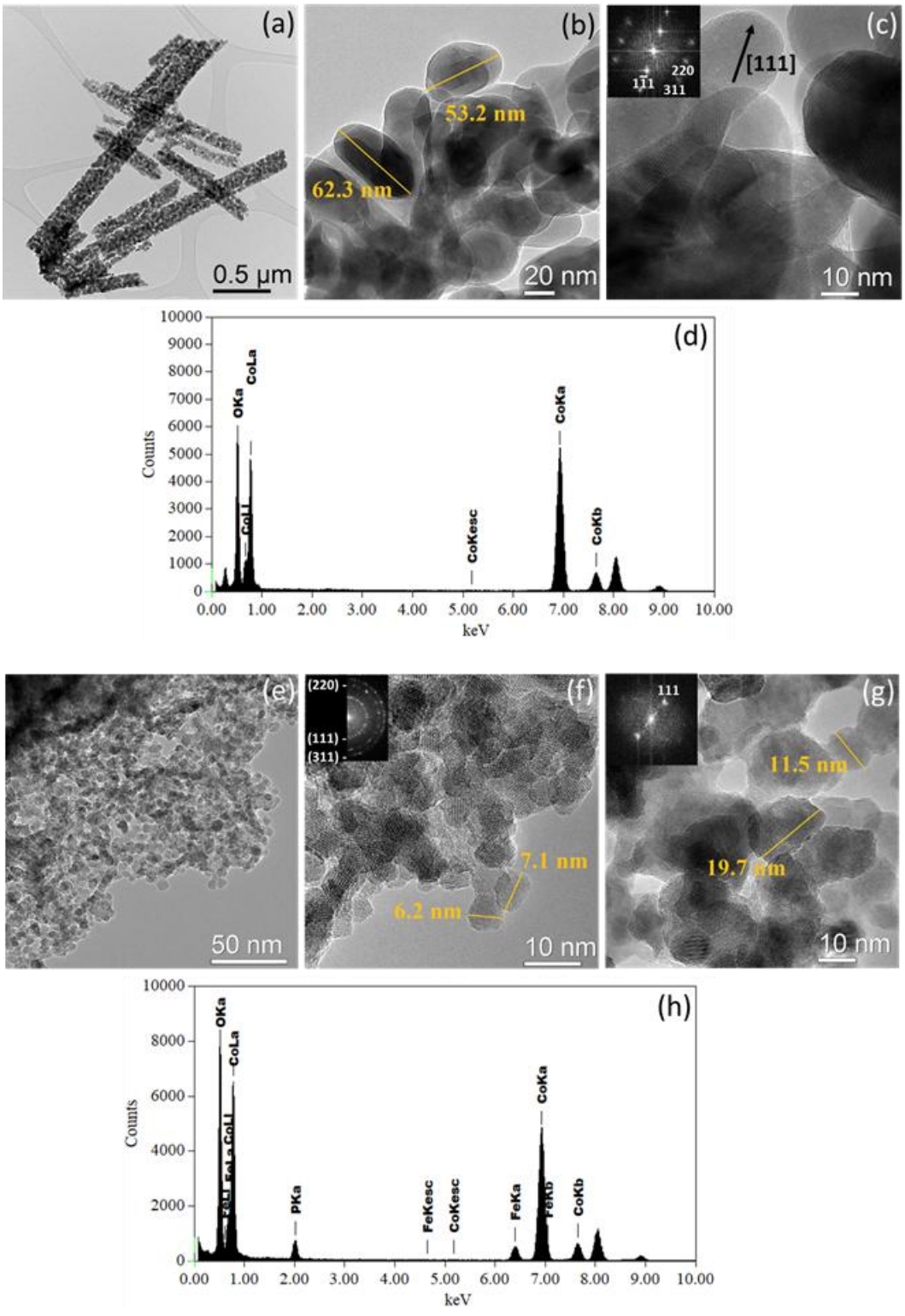

Figure 4: *TEM images of pristine Co_3O_4 (a-b) and sample CA-20 (e), high resolution TEM micrographs of pristine Co_3O_4 (c) and sample CA-20 (f-g) with corresponding Fast Fourier Transform (FFT) (in insert), EDS spectra for pristine Co_3O_4 (d) and sample CA-20 (h)*

Further information about the surface composition of the samples as well as the oxidation states of the elements on the surface was obtained from X-ray photoelectron spectroscopy (XPS). Figure 5 includes Co 2*p* and O 1*s* and core level spectra of pure Co_3O_4 and apple one (CA-20). The decomposition of Co 2*p* signal evidences five contributions (doublets) each one containing the Co $2p_{3/2}$ (solid line) and Co $2p_{1/2}$ (dotted line) with an intensity ratio 2:1. Pure Co_3O_4 sample shows the contributions typical of Co^{3+} at 779.8 eV, Co^{2+} at 781.5 eV, $Co(OH)_2$ at 782.6 eV and two broad contributions at higher binding energies due to shake-up satellites (surface and bulk plasmons) of cobalt ions, as observed in previous works [21,38,67] . The Co_3O_4 nanostructures (CA-20) sample shows the same contributions. However, the proportion Co^{3+}/Co^{2+} changes from 2.8 to 1.8 by including apple juice during the synthesis, i.e., the proportion of Co^{2+} ions is higher. Figure 5b shows O 1*s* signal, where three components are clearly noticeable at 529.7 eV, 531.5 eV and 532.7 eV, due to lattice oxygen related to Co-O bonds in cobalt spinel [66]; low coordination (O_2, O^{2-} and O^{-}) or surface oxygen species adsorbed over the surface oxygen vacancy (O_{Surf}); and chemisorbed oxygen (O_{Che}), respectively. By comparing both samples, O_{Surf}/O_{Lat} ratios changed from 0.36 to 0.69 for pristine Co_3O_4 and CA-20, respectively, indicating that CA-20 sample shows more oxygen vacancies on the surface probably associated due to an increase in the percentage of Co^{2+} ions on the surface. These are the surface atomic composition of CA-20 sample and observed results suggest that C1s, O1s, Fe2p, a Co2p and P2p25.16, 51.72, 0.18, 22.94 and 3.9 respectively. There is still room for the future studies to understand the induction of Fe and P into Co_3O_4 crystal arrays, and at the same time the oxidation states of P and Fe have to be studied. Furthermore, the XPS study has revealed the amount of oxygen vacancies and relative ratio of different oxidation states of Co which played together a significant role for driving OER reaction at low overpotential. The enhanced performance of sample CA-20 is mainly coming from the combined effects of crystal defects, variation in oxidation states of Co, transformation of morphology and addition of impurities of Fe and P.

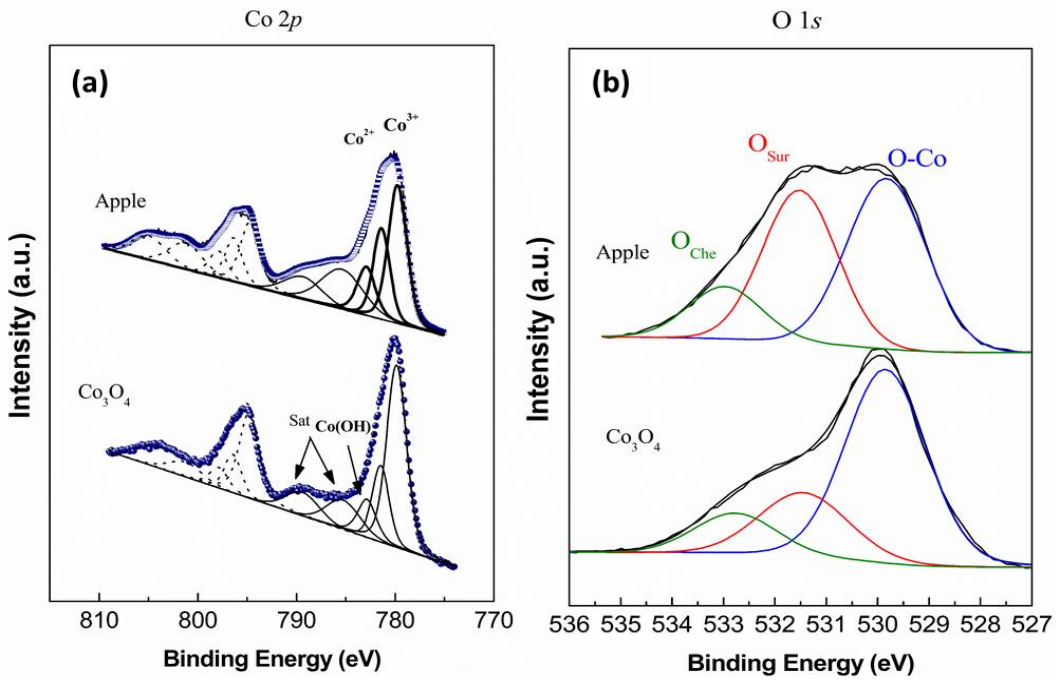

Figure 5: (a) *XPS spectra of Co-2p for pure Co_3O_4 and apple juice assisted Co_3O_4 nanostructures,* ***(b)*** *O-1s core level signals for pure Co_3O_4 and apple juice assisted Co_3O_4 nanostructures*

3.2. OER characterization onto surface modified Co_3O_4 nanostructures

The OER characterization was done with different surface modified Co_3O_4 nanostructures using linear sweep voltammetry (LSV) at scan rate of 1 mV/s in 1.0 M KOH electrolytic solution. For the comparison of pristine Co_3O_4 nanostructures and noble metal catalyst like RuO_2 were also studied under similar conditions. It was found during OER testing that each material exhibited has shown different value of overpotential like pristine Co_3O_4 (369 mV), RuO_2 (214 mV), CA-10 (330 mV), CA-20 (269 mV) and CA-30 (294 mV) as shown in Figure 6a. These overpotential values of various surface modified Co_3O_4 nanostructures suggest that rotten apple juice has drastically lowered the energy demand for OER process particularly for the sample CA-20 (269 mV). Importantly, the performance of CA-20 (269 mV) is not only related to rare doping of Fe and P but rotten apple juice is rich with variety of natural like reducing agents such as glucose, sucrose, starch, polyphenols and ascorbic acid which have effectively created the defects in the crystal structure Co_3O_4 nanostructures, and reduced the nanoparticle size as verified by XRD and TEM studies Furthermore, the EDX analysis with TEM has confirmed the presence of iron and phosphorous in the chemical composition of Co_3O_4 nanostructures, and they have played a

significant role in driving OER reaction at low energy demand. The surface science of Co_3O_4 nanostructures (CA-20) has revealed the high density of oxygen vacancies due to high concentration of Co^{2+} ions on the surface as confirmed by XPS analysis, therefore they have driven OER reaction relatively at low overpotential. The physical characterization of Co_3O_4 nanostructures (CA-20) evidently proved that the combined effects of reduced nanoparticle size, defects in the structure, presence of impurities of Fe and P and high density of oxygen vacancies together played a leading role towards increased OER performance. The biomolecules carried by the rotten apple juice are associated with high density of oxygenated groups which have driven effectively the surface modification of Co_3O_4 nanostructures as clearly seen by the SEM and HRTEM studies, consequently an enhanced OER activity was demonstrated. The sample CA-30 (294 mV) has shown relatively poor performance compare to the sample CA-20 due to two main reasons. The optimum volume of rotten apple juice was confirmed afterwards the use of rotten apple juice has limited the performance of as prepared Co_3O_4 nanostructures towards OER. The deactivation of sample CA-30 could be attributed to the removal of favorable surface for the OER after high amount of reducing agents from higher volume of rotten apple juice.

Additionally, the activity of noble metal catalyst is superior or close to the sample CA-20 (269 mV), however high cost of noble metal catalyst and rare abundance restrict its large scale applications but the newly developed, low cost, innovative and green approach for the surface modification of Co_3O_4 nanostructures can be used effectively for the complete exploitation of hydrogen gas from water splitting. The Tafel analysis was carried out on the obtained LSV OER polarization curves using Tafel equation for understanding the reaction kinetics as shown in Figure 6b. The Tafel calculation was done at using a linear range of LSV curve of particular catalytic material. The Tafel values for various samples were noticed as 55 $mVdec^{-1}$, 64 $mVdec^{-1}$, 85 $mVdec^{-1}$, 89 $mVdec^{-1}$, and 96 $mVdec^{-1}$ for RuO_2, CA-20, CA-30, CA-10, and pristine Co_3O_4 nanostructures respectively as shown in Figure 6b. The Tafel value of CA-20 is found close to noble catalyst, confirming that OER kinetics is highly favorable when surface of Co_3O_4 nanostructures was modified with certain chemical compounds present in the rotten apple juice. For the simplicity of representation of overpotential, a plot of overpotential of each material against 20 mA/cm^2 is enclosed in Figure 6c. The same overpotential value for the current density of 10 and 50 mA/cm^2 has also been done and shown in Figure S2.

Active surface area of each Co_3O_4 nanostructured material was also estimated using CV measurement at various scan rates as provided in (S1) using following relationship:

$$ECSA = C_{dl} / C_s \quad (4)$$

Where, Cs = 0.04 mF/cm^2 for KOH electrolyte [66,68].

A linear fit of ECSA against different scan rates is shown in Figure 6d, indicates that CA-20 sample is rich with surface active sites 510 cm^2as confirmed from the slope of linear fitting and its relative specific capacitance 20.4 $\mu F/cm^2$ was also observed higher compare to other samples. For the simplicity, the ECSA and specific capacitance values of all the catalytic materials are given in Table 1. The durability of CA-20 was performed to evaluate its features for long term application when it could, be used for the development of industrial water electrolyzer. For this purpose, we used a chronopotentiometry technique at constant current density 20 mA/cm^2 for the time period of 40 h as shown in Figure 6e. It is obvious that there was a negligible potential drop and the OER process could take place without any disturbance for the period of 40 h. The significantly enhanced durability might be attributed to the high compatible contact of Co_3O_4 material with GCE due to the use of mimic molecules from the rotten apple juice, uniform access of electron transport throughout the sample due to the surface modification of as prepared Co_3O_4 nanostructures with mimic environment of rotten apple juice. Moreover, we also studied the stability of (CA-20) material after the durability test using LSV measurement and obtained results confirm that the catalytic features of as prepared Co_3O_4 nanostructures are stable and can be used for long term applications as shown in Figure 6f.

The catalytic performance of newly prepared and rarely iron doped Co_3O_4 nanostructures is briefly described by onset potential as given in following order RuO_2 > CA-20 > CA-30 > CA-10 > Co_3O_4 at 20 mAcm^{-2} and the Tafel slopes order is shown as RuO_2 < CA-20 < < CA-30 < CA-10 < Co_3O_4 as enclosed in (Table 1).

The performance evaluation of Co_3O_4 nanostructures (CA-20) was compared with recently Co_3O_4 nanostructures based electrocatalyst as given in Table (S1). It is obvious that presented approach is simple, low cost, innovative, and green which confirms that methodology is useful and the performance of CA-20 sample is either equal or superior with respect to low energy demand and favorable reaction kinetics to many of the enclosed materials in Table (S1). In the presented study, we aimed to show the green approach for the use of surface modifying agents from rotten apple juice and addition of impurities of Fe and P into Co_3O_4 nanostructures for

driving the OER at low overpotential. Hence, we offer an alternative electrocatalyst based on surface modified Co_3O_4 nanostructures for the practical water catalysis.

.

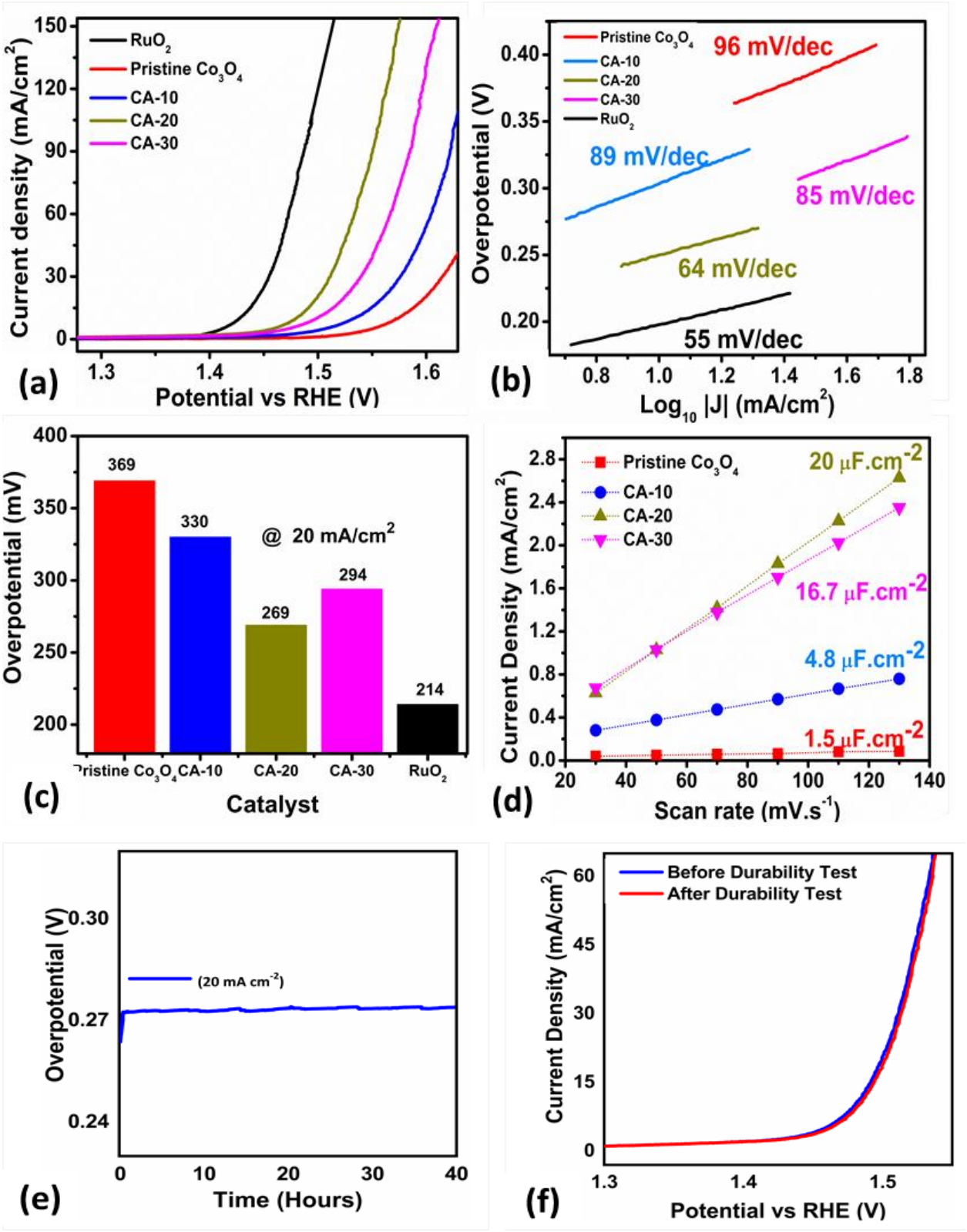

Figure 6: *(a) LSV polarization curves at a scan rate of 1 mV/s in 1.0 M KOH of RuO_2, pristine Co_3O_4, CA-10, CA-20 and CA-30. (b) Overpotential value chart (c). Tafel Plots in mV/dec. (d)*

Double Layer Capacitance values from CV curves at different scan rates. (e) Chronopotentiometry at 20mA/cm^2 current density for finding durability of the CA-20 for 40 hours at 1.39 V (versus RHE) in 1 M KOH. (f) LSV curve for checking stability of CA-20 before and after durable test.

The complete OER mechanism is not known yet, however a general approach have been used to represent the possible OER process onto the metal oxide nanostructures as shown in equation (5)

$$2H_2O = 4H^+ + O_2 + 4e^- \quad (5)$$

Furthermore, the Tafel analysis is used to describe the reaction intermediates involved in the OER as reported by [33], hence following sub steps which can be taken from equation (5) are used to show the generation of successful to reaction species as given below

$$M^* + OH^- = M^* - OH_{ads} + e^- \quad \text{Tafel slope value } >120 \quad (6)$$

$$M^* - OH_{ads} + OH^- = M^* - O_{ads}^- + H_2O \quad \text{Tafel slope value } 60 \quad (7)$$

$$M^* - O_{ads}^- = M^* - O_{ads} + e^- \quad \text{Tafel slope value } 40 \quad (8)$$

$$2\,M^* - O_{ads} = 2\,M^* + O_2\uparrow^- \quad \text{Tafel slope value } 15 \quad (9)$$

Based on the above sub reactions, we correlated the Taflel value oif CA-20 sample is well described by the sub step (7) for the occurrence of OER reaction onto rare iron doped Co_3O_4 nanostructures.

To have deep insight on the interface of electrode and electrode for the demonstration of charge transfer resistance, EIS measurement was done and supported by the possible of equivalent circuit using Z-view software as shown in Figure 7 a,b,c. The Nquist plots suggest that the surface modified Co_3O_4 nanostructures (CA-20) is experiencing a low charge transfer resistance of 118.9 Ω and high capacitance value of CPE_{cdl} 1.09 which verifies that the Co_3O_4 nanostructures exhibited high electrical conductivity and are highly efficient in producing the favorable interface chemistry via charge transfer as shown in Figure 7a. Additionally, we also identified that the sample CA-20 is associated with lower value of maximum oscillation

frequency (f_{max}) than others samples, revealing the sample CA-20 exhibits high electron recombination lifetime ($\tau_n = \frac{1}{2\pi f max}$), consequently high adsorption of reactive species onto the surface of CA-20 sample as shown in Bide plots Figure 7 b, c. The obtained values of charge transfer resistance, capacitance double layer from EIS data of pristine Co_3O_4, CA-10, CA-20 and CA-30 are enclosed in the Table 1. The EIS analysis strongly supports the claims made on the low energy demand, high ECSA values and low Tafel value of CA-20 sample for the foster OER process.

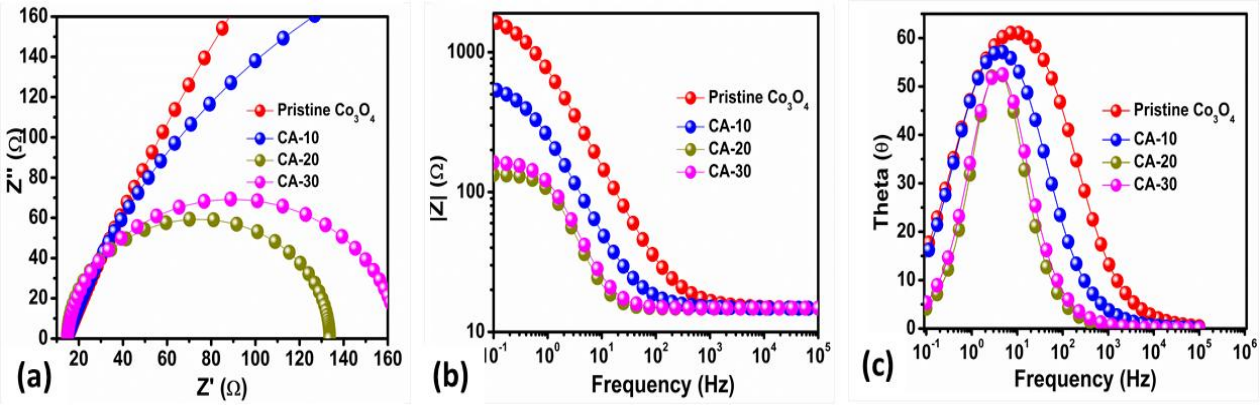

Figure 7: *Electrochemical impedance measurement in the frequency range from 0.1 Hz to 100 kHz in 1.0 M KOH with sinusoidal potential 10 mV and OER onset potential. (a) Nyquist plots for Pristine Co_3O_4, CA-10, CA-20 and CA-30. (b,c) for Bode plots I and II obtained from impedance data of Pristine Co_3O_4 CA-10, CA-20 and CA-30 nanoparticles.*

Table 1: A summary of obtained results from LSV, EIS and CV.

Catalyst	**Calculated from LSV**		**Calculated from EIS**		**Calculated from CV**	
	Over-potential	**Tafel Slope**	**Charge Transfer Resistance**	**Double Layer Capacitance**	**Double Layer Capacitance**	**Electrochemical active surface area**
	@ 20 mA/cm^2	***B***	R_{ct}	CPE_{cdl}	C_{dl}	***ECSA***
	mV	***mV/dec***	**Ω**	***mf***	***(μF/cm^2)***	***cm^2***
Pristine Co_3O_4	369	96	1924.0	0.21	1.5	37.5
CA-10	330	89	597.1	0.63	4.8	120.0

CA-20	**269**	**64**	**118.9**	**1.09**	**20.0**	**500.0**
CA-30	294	85	150.0	0.98	16.7	417.5

4. Conclusions

In summary, we have highly exploited the biomass waste of rotten apple juice for the surface modification of Co_3O_4 nanostructures using hydrothermal method. For the sake of optimization, different volumes of rotten apple juice were used to modify the surface properties of Co_3O_4. We have found a cubic crystal arrays of Co_3O_4 using XRD and TEM analysis. We have observed the presence of impurities of Fe and P into Co_3O_4 nanostructures. A surface oxygen vacancies and mixed oxidation states of cobalt into the Co_3O_4 sample (CA) strongly enhanced the OER activity with a low energy demand of 269 mV. Moreover, the optimized sample Co_3O_4 (CA-20) was further well characterized by low Tafel slope of 64 $mVdec^{-1}$ and high durability of 40 h. The superior performance of Co_3O_4 nanostructures (sample CA-20) was attributed from the rich amount of catalytic sites, impurities of Fe and P, enhanced electrical conductivity, low charge transfer resistance, large oxygen vacancies, reduced particle size, defects in the structure, and tuned surface properties by the wide range of natural reducing agents available in the rotten apple juice. After the performance of sample CA-20, it is safe to say that newly approach can be of high interest for the design of new generation of electrocatalysts for the wide range of applications including water splitting, batteries and fuel cell technology.

Acknowledgment

We would like to thank the platform "Microscopies, Microprobes and Metallography (3M)" (Institut Jean Lamour, IJL, Nancy, France) for TEM and SEM facilities. A.I.M. acknowledges RTI2018-099668-BC22, RyC-2015-17870 and UMA18-FEDERJA-126 projects (Spain). The authors also express their gratitude to the support of Princess Nourah bint Abdulrahman University Researchers Supporting Project number (PNURSP2022R58), Princess Nourah bint Abdulrahman University, Riyadh, Saudi Arabia

Declaration of interest

Authors declare no conflict of interest in this research work

Data Availability Statement

The datasets generated analyzed during the current study are available from the corresponding author on reasonable request

5. References:

[1] B. Looney, Statistical Review of World Energy globally consistent data on world energy markets . and authoritative publications in the field of energy, Rev. World Energy Data. 70 (2021) 8–20.

[2] U.N.G. Assembly, Transforming our world: the 2030 agenda for sustainable development, 21 October 2015, A/RES/70/1, 2015.

[3] S. Mondal, A.K. Mondal, V. Chintala, S.M. Tauseef, S. Kumar, J.K. Pandey, Thermochemical pyrolysis of biomass using solar energy for efficient biofuel production: a review, Biofuels. 12 (2021) 125–134. https://doi.org/10.1080/17597269.2018.1461512.

[4] V. Sebestyén, Renewable and Sustainable Energy Reviews: Environmental impact networks of renewable energy power plants, Renew. Sustain. Energy Rev. 151 (2021) 111626. https://doi.org/10.1016/j.rser.2021.111626.

[5] M. El Haj Assad, S. Zubayda, B. Khuwaileh, A. Hmida, M. Al-Shabi, Geothermal energy as power producer, 11722 (2021) 28. https://doi.org/10.1117/12.2586263.

[6] A.T. Hoang, S. Nizetic, H.C. Ong, C.T. Chong, A.E. Atabani, V.V. Pham, Acid-based lignocellulosic biomass biorefinery for bioenergy production: Advantages, application constraints, and perspectives, J. Environ. Manage. 296 (2021) 113194. https://doi.org/10.1016/j.jenvman.2021.113194.

[7] S. Chen, M. Li, M. Gao, J. Jin, M. A. van Spronsen, M. B. Salmeron, P. Yang, High-Performance Pt–Co Nanoframes for Fuel-Cell Electrocatalysis, Nano Lett. 20 (2020) 1974–1979. https://doi.org/10.1021/acs.nanolett.9b05251.

[8] B. Sundén, Fuel cell systems and applications, Hydrog. Batter. Fuel Cells. (2019) 203–216. https://doi.org/10.1016/b978-0-12-816950-6.00011-7.

[9] B. Sundén, Fuel cell types - overview, Hydrog. Batter. Fuel Cells. (2019) 123–144. https://doi.org/10.1016/b978-0-12-816950-6.00008-7.

[10] A.G. Olabi, T. Wilberforce, M.A. Abdelkareem, Fuel cell application in the automotive industry and future perspective, Energy. 214 (2021) 118955. https://doi.org/10.1016/j.energy.2020.118955.

[11] B. Sundén, Transport phenomena in fuel cells, Hydrog. Batter. Fuel Cells. (2019) 145–166. https://doi.org/10.1016/b978-0-12-816950-6.00009-9.

[12] J. Lindorfer, D.C. Rosenfeld, H. Böhm, Fuel cells: Energy conversion technology,

Elsevier Ltd, 2020. https://doi.org/10.1016/B978-0-08-102886-5.00023-2.

[13] T. Capurso, M. Stefanizzi, M. Torresi, S.M. Camporeale, Perspective of the role of hydrogen in the 21st century energy transition, Energy Convers. Manag. 251 (2022) 114898. https://doi.org/10.1016/j.enconman.2021.114898.

[14] C.J. Winter, Hydrogen energy - Abundant, efficient, clean: A debate over the energy-system-of-change, Int. J. Hydrogen Energy. 34 (2009) 1–52. https://doi.org/10.1016/j.ijhydene.2009.05.063.

[15] J. Brauns, T. Turek, Alkaline water electrolysis powered by renewable energy: A review, Processes. 8 (2020). https://doi.org/10.3390/pr8020248.

[16] D. Wu, K. Kusada, S. Yoshioka, T. Yamamoto, T. Toriyama, S. Matsumura, Y. Chen, O. Seo, J. Kim, C. Song, S. Hiroi, O. Sakata, T. Ina, S. Kawaguchi, Y. Kubota, H. Kobayashi, H. Kitagawa, Efficient overall water splitting in acid with anisotropic metal nanosheets, Nat. Commun. 12 (2021) 1–9. https://doi.org/10.1038/s41467-021-20956-4.

[17] S.M. Ibn Shamsah, Earth-abundant electrocatalysts for water splitting: Current and future directions, Catalysts. 11 (2021). https://doi.org/10.3390/catal11040429.

[18] K. Harrison, J.I. Levene, Electrolysis of water using hydrogen sulfide, Int. J. Hydrogen Energy. 16 (1991) 503–503. https://doi.org/10.1016/0360-3199(91)90107-t.

[19] S. Wang, A. Lu, C.J. Zhong, Hydrogen production from water electrolysis : role of catalysts, Nano Converg. (2021). https://doi.org/10.1186/s40580-021-00254-x.

[20] J.D. Holladay, J. Hu, D.L. King, Y. Wang, An overview of hydrogen production technologies, Catal. Today. 139 (2009) 244–260. https://doi.org/10.1016/j.cattod.2008.08.039.

[21] M.Y. Solangi, U. Aftab, A. Tahira, M.I. Abro, R. Mazarro, V. Morandi, A. Nafady, S.S. Medany, A. Infantes-Molina, Z.H. Ibupoto, An efficient palladium oxide nanoparticles@Co3O4 nanocomposite with low chemisorbed species for enhanced oxygen evolution reaction, Int. J. Hydrogen Energy. 47 (2022) 3834–3845. https://doi.org/10.1016/j.ijhydene.2021.11.042.

[22] W.Z. Li, M.Y. Liu, L. Gong, M.L. Zhang, C. Cao, Y. He, The electronic properties and catalytic activity of precious-metals adsorbed silicene for hydrogen evolution reaction and oxygen evolution reaction, Appl. Surf. Sci. 560 (2021) 150041. https://doi.org/10.1016/j.apsusc.2021.150041.

[23] F.A.L. Laskowski, M.R. Nellist, J. Qiu, S.W. Boettcher, Metal Oxide/(oxy)hydroxide Overlayers as Hole Collectors and Oxygen-Evolution Catalysts on Water-Splitting Photoanodes, J. Am. Chem. Soc. 141 (2019) 1394–1405. https://doi.org/10.1021/jacs.8b09449.

[24] A. Dutta, N. Pradhan, Developments of Metal Phosphides as Efficient OER Precatalysts, J. Phys. Chem. Lett. 8 (2017) 144–152. https://doi.org/10.1021/acs.jpclett.6b02249.

[25] D.W. Wang, D. Su, Heterogeneous nanocarbon materials for oxygen reduction reaction, Energy Environ. Sci. 7 (2014) 576–591. https://doi.org/10.1039/c3ee43463j.

[26] B.M. Hunter, H.B. Gray, A.M. Müller, Earth-Abundant Heterogeneous Water Oxidation Catalysts, Chem. Rev. 116 (2016) 14120–14136. https://doi.org/10.1021/acs.chemrev.6b00398.

[27] M. Tahir, L. Pan, F. Idrees, X. Zhang, L. Wang, J.J. Zou, Z.L. Wang, Electrocatalytic oxygen evolution reaction for energy conversion and storage: A comprehensive review, Nano Energy. 37 (2017) 136–157. https://doi.org/10.1016/j.nanoen.2017.05.022.

[28] Z.H. Ibupoto, A. Tahira, A.A. Shah, U. Aftab, M.Y. Solangi, J.A. Leghari, A.H. Samoon, A.L. Bhatti, M.A. Bhatti, R. Mazzaro, V. Morandi, M.I. Abro, A. Nafady, A.M. Al-Enizi, M. Emo, B. Vigolo, NiCo2O4 nanostructures loaded onto pencil graphite rod: An advanced composite material for oxygen evolution reaction, Int. J. Hydrogen Energy. 47 (2022) 6650–6665. https://doi.org/10.1016/j.ijhydene.2021.12.024.

[29] C. Huang, P. Qin, Y. Luo, Q. Ruan, L. Liu, Y. Wu, Q. Li, Y. Xu, R. Liu, P.K. Chu, Recent progress and perspective of cobalt-based catalysts for water splitting: design and nanoarchitectonics, Mater. Today Energy. 23 (2022) 100911. https://doi.org/10.1016/j.mtener.2021.100911.

[30] E. Loni, A. Shokuhfar, M.H. Siadati, Cobalt-Based Electrocatalysts for Water Splitting: An Overview, Catal. Surv. from Asia. 25 (2021) 114–147. https://doi.org/10.1007/s10563-021-09329-5.

[31] B.-Y. Guo, X. Zhang, X. Ma, T.-S. Chen, Y. Chen, M. Wen, J. Qin, J. Nan, Y. Chai, B. Dong, RuO2/Co3O4 Nanocubes based on Ru ions impregnation into prussian blue precursor for oxygen evolution, Int. J. Hydrogen Energy. 45 (2020) 9575–9582.

[32] U. Aftab, A. Tahira, R. Mazzaro, M.I. Abro, M.M. Baloch, M. Willander, O. Nur, C. Yu, Z.H. Ibupoto, The chemically reduced CuO-Co3O4 composite as a highly efficient

electrocatalyst for oxygen evolution reaction in alkaline media, Catal. Sci. Technol. 9 (2019) 6274–6284. https://doi.org/10.1039/c9cy01754b.

[33] U. Aftab, A. Tahira, A. Gradone, V. Morandi, M.I. Abro, M.M. Baloch, A.L. Bhatti, A. Nafady, A. Vomiero, Z.H. Ibupoto, Two step synthesis of TiO2–Co3O4 composite for efficient oxygen evolution reaction, Int. J. Hydrogen Energy. 46 (2021) 9110–9122. https://doi.org/10.1016/j.ijhydene.2020.12.204.

[34] U. Aftab, A. Tahira, A.H. Samo, M.I. Abro, M.M. Baloch, M. Kumar, Sirajuddin, Z.H. Ibupoto, Mixed CoS2@Co3O4 composite material: An efficient nonprecious electrocatalyst for hydrogen evolution reaction, Int. J. Hydrogen Energy. 45 (2020) 13805–13813. https://doi.org/10.1016/j.ijhydene.2020.03.131.

[35] E. Fabbri, A. Habereder, K. Waltar, R. Kötz, T.J. Schmidt, Developments and perspectives of oxide-based catalysts for the oxygen evolution reaction, Catal. Sci. Technol. 4 (2014) 3800–3821. https://doi.org/10.1039/c4cy00669k.

[36] S. Cosentino, M. Urso, G. Torrisi, S. Battiato, F. Priolo, A. Terrasi, S. Mirabella, High intrinsic activity of the oxygen evolution reaction in low-cost NiO nanowall electrocatalysts, Mater. Adv. 1 (2020) 1971–1979. https://doi.org/10.1039/d0ma00467g.

[37] U. Aftab, A. Tahira, R. Mazzaro, V. Morandi, M.I. Abro, M.M. Baloch, J.A. Syed, A. Nafady, Z.H. Ibupoto, Facile NiCo2S4/C nanocomposite: an efficient material for water oxidation, Tungsten. 2 (2020) 403–410. https://doi.org/10.1007/s42864-020-00066-2.

[38] A.J. Laghari, U. Aftab, A. Tahira, A.A. Shah, A. Gradone, M.Y. Solangi, A.H. Samo, M. kumar, M.I. Abro, M. wasim Akhtar, R. Mazzaro, V. Morandi, A.M. Alotaibi, A. Nafady, A. Infantes-Molina, Z.H. Ibupoto, MgO as promoter for electrocatalytic activities of Co3O4–MgO composite via abundant oxygen vacancies and Co2+ ions towards oxygen evolution reaction, Int. J. Hydrogen Energy. (2022). https://doi.org/10.1016/J.IJHYDENE.2022.04.169.

[39] K.A.S. Usman, J.W. Maina, S. Seyedin, M.T. Conato, L.M. Payawan, L.F. Dumée, J.M. Razal, Downsizing metal–organic frameworks by bottom-up and top-down methods, NPG Asia Mater. 12 (2020). https://doi.org/10.1038/s41427-020-00240-5.

[40] M. Th. Makhlouf, B. M. Abu-Zied, T. H. Mansoure, Direct Fabrication of Cobalt Oxide Nano-particles Employing Glycine as a Combustion Fuel, Phys. Chem. 2 (2013) 86–93. https://doi.org/10.5923/j.pc.20120206.01.

[41] B. Chang, Z. Gu, Y. Guo, Z. Li, B. Yang, Glucose-assisted synthesis of Co3O4 nanostructure with controllable morphologies from nanosheets to nanowires, J. Alloys Compd. 676 (2016) 26–36. https://doi.org/10.1016/j.jallcom.2016.03.056.

[42] M.T. Makhlouf, B.M. Abu-Zied, T.H. Mansoure, Direct Fabrication of Cobalt Oxide Nanoparticles Employing Sucrose as a Combustion Fuel, J. Nanoparticles. 2013 (2013) 1–7. https://doi.org/10.1155/2013/384350.

[43] A. Tahira, A. Nafady, Q. Baloach, Sirajuddin, S.T.H. Sherazi, T. Shaikh, M. Arain, M. Willander, Z.H. Ibupoto, Ascorbic Acid Assisted Synthesis of Cobalt Oxide Nanostructures, Their Electrochemical Sensing Application for the Sensitive Determination of Hydrazine, J. Electron. Mater. 45 (2016) 3695–3701. https://doi.org/10.1007/s11664-016-4547-9.

[44] B. Jiang, Y. Guo, J. Kim, A.E. Whitten, K. Wood, K. Kani, A.E. Rowan, J. Henzie, Y. Yamauchi, Mesoporous Metallic Iridium Nanosheets, J. Am. Chem. Soc. 140 (2018) 12434–12441. https://doi.org/10.1021/jacs.8b05206.

[45] M.A. Rahman, R. Radhakrishnan, R. Gopalakrishnan, Structural, optical, magnetic and antibacterial properties of Nd doped NiO nanoparticles prepared by co-precipitation method, J. Alloys Compd. (2018). https://doi.org/10.1016/j.jallcom.2018.01.298.

[46] P.G. Jamkhande, N.W. Ghule, A.H. Bamer, M.G. Kalaskar, Metal nanoparticles synthesis: An overview on methods of preparation, advantages and disadvantages, and applications, J. Drug Deliv. Sci. Technol. 53 (2019). https://doi.org/10.1016/j.jddst.2019.101174.

[47] M.A. Islam, M. V. Jacob, E. Antunes, A critical review on silver nanoparticles: From synthesis and applications to its mitigation through low-cost adsorption by biochar, J. Environ. Manage. 281 (2021) 111918. https://doi.org/10.1016/j.jenvman.2020.111918.

[48] F. Moradnia, S. Taghavi Fardood, A. Ramazani, B. ki Min, S.W. Joo, R.S. Varma, Magnetic Mg0.5Zn0.5FeMnO4 nanoparticles: Green sol-gel synthesis, characterization, and photocatalytic applications, J. Clean. Prod. 288 (2021) 125632. https://doi.org/10.1016/j.jclepro.2020.125632.

[49] P. Singh, Y.J. Kim, D. Zhang, D.C. Yang, Biological Synthesis of Nanoparticles from Plants and Microorganisms, Trends Biotechnol. 34 (2016) 588–599. https://doi.org/10.1016/j.tibtech.2016.02.006.

[50] S. Jadoun, R. Arif, N.K. Jangid, R.K. Meena, Green synthesis of nanoparticles using plant

extracts: a review, Environ. Chem. Lett. 19 (2021) 355–374. https://doi.org/10.1007/s10311-020-01074-x.

[51] S.S. Salem, A. Fouda, Green Synthesis of Metallic Nanoparticles and Their Prospective Biotechnological Applications: an Overview, Biol. Trace Elem. Res. 199 (2021) 344–370. https://doi.org/10.1007/s12011-020-02138-3.

[52] S.S. Shankar, A. Rai, B. Ankamwar, A. Singh, A. Ahmad, M. Sastry, Biological synthesis of triangular gold nanoprisms, Nat. Mater. 3 (2004) 482–488. https://doi.org/10.1038/nmat1152.

[53] M. Hafeez, R. Shaheen, B. Akram, Zain-Ul-Abdin, S. Haq, S. Mahsud, S. Ali, R.T. Khan, Green synthesis of cobalt oxide nanoparticles for potential biological applications, Mater. Res. Express. 7 (2020). https://doi.org/10.1088/2053-1591/ab70dd.

[54] K. Chand, M.I. Abro, U. Aftab, A.H. Shah, M.N. Lakhan, D. Cao, G. Mehdi, A.M. Ali Mohamed, Green synthesis characterization and antimicrobial activity against: Staphylococcus aureus of silver nanoparticles using extracts of neem, onion and tomato, RSC Adv. 9 (2019) 17002–17015. https://doi.org/10.1039/c9ra01407a.

[55] F. Ortega, V.B. Arce, M.A. Garcia, Nanocomposite starch-based films containing silver nanoparticles synthesized with lemon juice as reducing and stabilizing agent, Carbohydr. Polym. 252 (2021). https://doi.org/10.1016/j.carbpol.2020.117208.

[56] A.M. El Shafey, Green synthesis of metal and metal oxide nanoparticles from plant leaf extracts and their applications: A review, Green Process. Synth. 9 (2020) 304–339. https://doi.org/10.1515/gps-2020-0031.

[57] M. Saeed, N. Akram, S. Ali, R. Naqvi, M. Usman, M.A. Abbas, Self-dual Leonard pairs Green and eco-friendly synthesis of Co a O, (2019) 382–390.

[58] N. Akhlaghi, G. Najafpour-Darzi, H. Younesi, Facile and green synthesis of cobalt oxide nanoparticles using ethanolic extract of Trigonella foenumgraceum (Fenugreek) leaves, Adv. Powder Technol. 31 (2020) 3562–3569. https://doi.org/10.1016/j.apt.2020.07.004.

[59] M.S. Samuel, E. Selvarajan, T. Mathimani, N. Santhanam, T.N. Phuong, K. Brindhadevi, A. Pugazhendhi, Green synthesis of cobalt-oxide nanoparticle using jumbo Muscadine (Vitis rotundifolia): Characterization and photo-catalytic activity of acid Blue-74, J. Photochem. Photobiol. B Biol. 211 (2020) 112011. https://doi.org/10.1016/j.jphotobiol.2020.112011.

[60] R. Noor, H. Yasmin, N. Ilyas, A. Nosheen, M.N. Hassan, S. Mumtaz, N. Khan, A. Ahmad, P. Ahmad, Comparative analysis of iron oxide nanoparticles synthesized from ginger (Zingiber officinale) and cumin seeds (Cuminum cyminum) to induce resistance in wheat against drought stress, Chemosphere. 292 (2022) 133201. https://doi.org/10.1016/j.chemosphere.2021.133201.

[61] Y. Rashtbari, F. Sher, S. Afshin, A. Hamzezadeh bahrami, S. Ahmadi, O. Azhar, A. Rastegar, S. Ghosh, Y. Poureshgh, Green synthesis of zero-valent iron nanoparticles and loading effect on activated carbon for furfural adsorption, Chemosphere. 287 (2022) 132114. https://doi.org/10.1016/j.chemosphere.2021.132114.

[62] T. Iqbal, A. Raza, M. Zafar, S. Afsheen, I. Kebaili, H. Alrobei, Plant-mediated green synthesis of zinc oxide nanoparticles for novel application to enhance the shelf life of tomatoes, Appl. Nanosci. 12 (2022) 179–191. https://doi.org/10.1007/s13204-021-02238-z.

[63] M. Rafique, R. Tahir, S.S.A. Gillani, M.B. Tahir, M. Shakil, T. Iqbal, M.O. Abdellahi, Plant-mediated green synthesis of zinc oxide nanoparticles from Syzygium Cumini for seed germination and wastewater purification, Int. J. Environ. Anal. Chem. 102 (2022) 23–38. https://doi.org/10.1080/03067319.2020.1715379.

[64] N.M. Rendtorff, M.S. Conconi, E.F. Aglietti, C.Y. Chain, A.F. Pasquevich, P.C. Rivas, J.A. Martínez, M.C. Caracoche, Phase quantification of mullite-zirconia and zircon commercial powders using PAC and XRD techniques, Hyperfine Interact. 198 (2010) 211–218. https://doi.org/10.1007/s10751-010-0177-4.

[65] A. Yamuna, T.W. Chen, S.M. Chen, Synthesis and characterizations of iron antimony oxide nanoparticles and its applications in electrochemical detection of carbendazim in apple juice and paddy water samples, Food Chem. 373 (2022) 131569. https://doi.org/10.1016/j.foodchem.2021.131569.

[66] X. Shang, K.L. Yan, Y. Rao, B. Dong, J.Q. Chi, Y.R. Liu, X. Li, Y.M. Chai, C.G. Liu, In situ cathodic activation of V-incorporated NixSy nanowires for enhanced hydrogen evolution, 2017. https://doi.org/10.1039/c7nr02867a.

[67] A.L. Bhatti, A. Tahira, A. Gradone, R. Mazzaro, V. Morandi, U. aftab, M.I. Abro, A. Nafady, K. Qi, A. Infantes-Molina, A. Vomiero, Z.H. Ibupoto, Nanostructured Co3O4 electrocatalyst for OER: The role of organic polyelectrolytes as soft templates,

Electrochim. Acta. 398 (2021) 139338. https://doi.org/10.1016/j.electacta.2021.139338.

[68] H.S. Jadhav, A. Roy, G.M. Thorat, W.J. Chung, J.G. Seo, Hierarchical free-standing networks of MnCo2S4 as efficient Electrocatalyst for oxygen evolution reaction, J. Ind. Eng. Chem. 71 (2019) 452–459. https://doi.org/10.1016/j.jiec.2018.12.002.

Surface modification of Co_3O_4 nanostructures using wide range of natural compounds from rotten apple juice for the efficient oxygen evolution reaction

Abdul Jaleel Laghari[a], Umair Aftab[a], Aqeel Ahmed Shah[c], Muhammad Yameen Solangi[a], Muhammad Ishaque Abro[a], Sameerah I. Al-Saeedi[h], Noha Naeim[f], Ayman Nafady[g], Brigitte Vigolo[d], Melanie Emo[d], Antonia Infantes Molina[e], Aneela Tahira[b], Zafar Hussain Ibhupoto[b]*

[a]Department of Metallurgy and Materials Engineering, Mehran University of Engineering and Technology, 76080 Jamshoro, Sindh Pakistan

[b]Dr. M.A Kazi Institute of Chemistry University of Sindh Jamshoro, 76080, Sindh Pakistan

[c]Department of Metallurgy, NED university of Engineering and Technology, Karachi Pakistan

[d]Université de Lorraine, CNRS, IJL, F-54000 Nancy, France

[e]Department of Inorgnic Chemistry, Crystallography and Mineralogy. (Unidad Asociada al ICP-CSIC), Faculty of Sciences, University of Malaga, Campus de Teatinos, 29071 Malaga, Spain France

[f]Department of Production Engineering and Mechanical Design, Port Said University, Port Fua, 42526, Egypt

[g]Department of Chemistry, College of Science, King Saud University, Riyadh 11451, Saudi Arabia

[h]Department of Chemistry, College of Science, Princess Nourah bint Abdulrahman University, P.O.Box 84428, Riyadh 11671, Saudi Arabia

Corresponding authors: Zafar Hussian Ibupoto, PhD*, Email address: zaffar.ibhupoto@usindh.edu.pk

Supplementary information

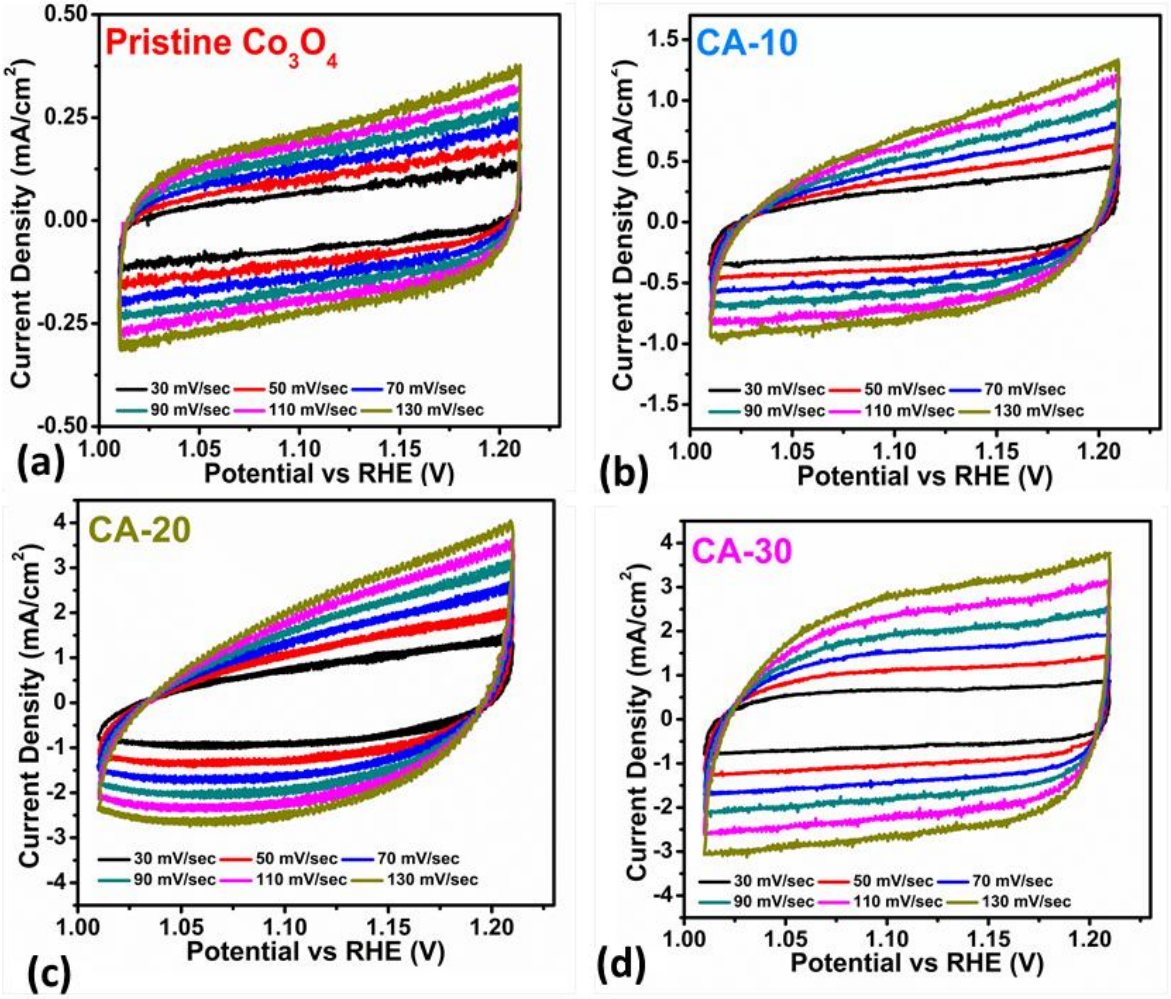

Fig. S1. *CV curves at various scan rates (a) pristine Co_3O_4 (b) CA-10 (c) CA-20, (d) CA-30*

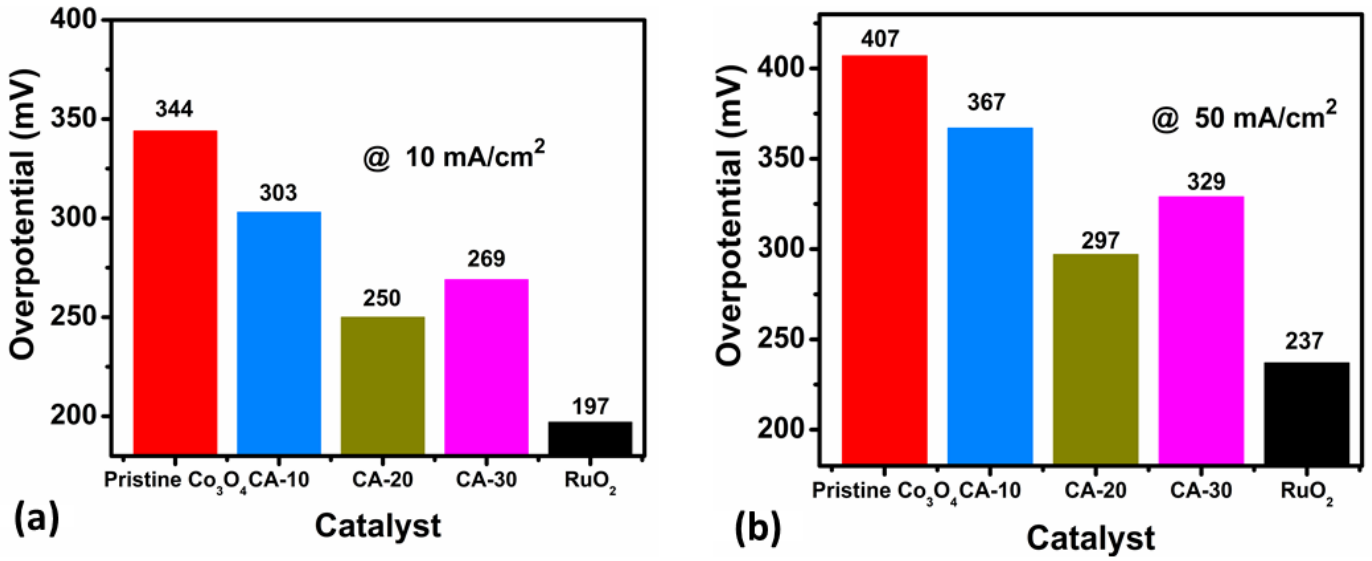

Fig. S2. *(a) Overpotential value chart at current density of 10 mA/cm^2 and (b) at 50 mA/cm^2 calculated from LSV polarization curves.*

Table S2. *Comparison of CA-20 nanoparticles as OER electrocatalysts with recently reported electrocatalysts.*

Electrocatalyst	**Electrolyte**	**Current Density**	**Overpotential**	**Tafel Slope**	**Reference**
CA-20	1 M KOH	20 mA cm^{-2}	269 mV	64 mV dec^{-1}	This work
MgO-Co_3O_4	1 M KOH	10 mA cm^{-2}	274 mV	64 mV dec^{-1}	[1]
Fe_3O_4 -Co_3O_4	1 M KOH	10 mA cm^{-2}	370 mV	80 mV dec^{-1}	[2]
CdO - Co_3O_4	1 M KOH	10 mA cm^{-2}	310 mV	62 mV dec^{-1}	[3]
CuO-Co_3O_4	1 M KOH	40 mA cm^{-2}	144 mV	74 mV dec^{-1}	[4]
$CoFe_2O_4$/graphene	1 M KOH	10 mA cm^{-2}	300 mV	68 mV dec^{-}	[5]
TiO_2-Co_3O_4	1 M KOH	10 mA cm^{-2}	270 mV	60 mV dec^{-1}	[6]
Co_3O_{4-x}-C@Fe_2–y$Co_yO_{3\backslash}$	1 M KOH	10 mA cm^{-2}	290 mV	37.6 mV dec^{-1}	[7]
Ni - Co_3O_4	1 M KOH	10 mA cm^{-2}	300 mV	82 mV dec^{-1}	[8]
Co_3O_4@Co	1 M KOH	10 mA cm^{-2}	273 mV	61.8 mV dec^{-1}	[9]

References:

[1] A.J. Laghari, U. Aftab, A. Tahira, A.A. Shah, A. Gradone, M.Y. Solangi, A.H. Samo, M. kumar, M.I. Abro, M. wasim Akhtar, R. Mazzaro, V. Morandi, A.M. Alotaibi, A. Nafady, A. Infantes-Molina, Z.H. Ibupoto, MgO as promoter for electrocatalytic activities of Co3O4–MgO composite via abundant oxygen vacancies and Co2+ ions towards oxygen evolution reaction, Int. J. Hydrogen Energy. (2022). https://doi.org/10.1016/J.IJHYDENE.2022.04.169.

[2] A.L. Bhatti, U. Aftab, A. Tahira, M.I. Abro, R.H. Mari, M.K. Samoon, M.H. Aghem, N.M. Shaikh, A.Q. Mugheri, Z.H. Ibupoto, An Efficient and Functional Fe_3O_4 /Co_3O_4 Composite for Oxygen Evolution Reaction., J. Nanosci. Nanotechnol. 21 (2021) 2675–2680. https://doi.org/10.1166/jnn.2021.19098.

[3] A. Hanan, A.J. Laghari, M.Y. Solangi, U. Aftab, M.I. Abro, D. Cao, M. Ahmed, M.N. Lakhan, A. Ali, A. Asif, A.H. Shar, Cdo/Co3O4 Nanocomposite As an Efficient Electrocatalyst for Oxygen Evolution Reaction in Alkaline Media, Int. J. Eng. Sci. Technol. 6 (2022) 1–10. https://doi.org/10.29121/ijoest.v6.i1.2022.259.

[4] U. Aftab, A. Tahira, R. Mazzaro, M.I. Abro, M.M. Baloch, M. Willander, O. Nur, C. Yu, Z.H. Ibupoto, The chemically reduced CuO-Co3O4 composite as a highly efficient electrocatalyst for oxygen evolution reaction in alkaline media, Catal. Sci. Technol. 9 (2019) 6274–6284. https://doi.org/10.1039/c9cy01754b.

[5] Y. Ma, H. Zhang, J. Xia, Z. Pan, X. Wang, G. Zhu, B. Zheng, G. Liu, L. Lang, Reduced CoFe2O4/graphene composite with rich oxygen vacancies as a high efficient electrocatalyst for oxygen evolution reaction, Int. J. Hydrogen Energy. 45 (2020) 11052–11061. https://doi.org/10.1016/j.ijhydene.2020.02.045.

[6] U. Aftab, A. Tahira, A. Gradone, V. Morandi, M.I. Abro, M.M. Baloch, A.L. Bhatti, A. Nafady, A. Vomiero, Z.H. Ibupoto, Two step synthesis of TiO2–Co3O4 composite for efficient oxygen evolution reaction, Int. J. Hydrogen Energy. 46 (2021) 9110–9122. https://doi.org/10.1016/j.ijhydene.2020.12.204.

[7] W. Xu, W. Xie, Y. Wang, Co3O4-x-Carbon@Fe2-yCoyO3 Heterostructural Hollow Polyhedrons for the Oxygen Evolution Reaction, ACS Appl. Mater. Interfaces. 9 (2017) 28642–28649. https://doi.org/10.1021/acsami.7b09213.

[8] A.L. Bhatti, U. Aftab, A. Tahira, M.I. Abro, M. Kashif Samoon, M.H. Aghem, M.A. Bhatti, Z. Hussainibupoto, Facile doping of nickel into Co3O4 nanostructures to make them efficient for catalyzing the oxygen evolution reaction, RSC Adv. 10 (2020) 12962–12969. https://doi.org/10.1039/d0ra00441c.

[9] L. Zhang, Q. Liang, P. Yang, Y. Huang, W. Chen, X. Deng, H. Yang, J. Yan, Y. Liu, Flower-like Co3O4 microstrips embedded in Co foam as a binder-free electrocatalyst for oxygen evolution reaction, Int. J. Hydrogen Energy. 44 (2019) 24209–24217. https://doi.org/10.1016/j.ijhydene.2019.07.146.